

1 **Future applications of hydrogen production and CO₂**
2 **utilization for energy storage: Hybrid Power to Gas-**
3 **Oxycombustion power plants**

4 **Manuel BAILERA^a, Nouaamane KEZIBRI^b, Luis M. ROMEO^{a*}, Sergio ESPATOLERO^c,**
5 **Pilar LISBONA^d, Chakib BOUALLOU^b**

6 ^a Escuela de Ingeniería y Arquitectura. Departamento de Ingeniería Mecánica. Universidad de Zaragoza,
7 Campus Río Ebro, María de Luna 3, 50018, Zaragoza, Spain

8 ^b Centre Efficacité énergétique des Systèmes (CES) - Center for Energy efficiency of Systems,
9 5 Rue Léon Blum, 91120, Palaiseau, France

10 ^c Research Centre for Energy Resources and Consumption (CIRCE),
11 CIRCE Building – Campus Río Ebro, Mariano Esquillor Gómez, 15, 50018, Zaragoza, Spain

12 ^d Escuela Universitaria de Ingenierías Agrarias de Soria - Universidad de Valladolid,
13 Campus Universitario Duques de Soria, 42004, Soria, Spain.

14
15 **Abstract**

16 Power to Gas (PtG) has appeared in the last years as a potential long-term energy storage
17 solution, which converts hydrogen produced by renewable electricity surplus into synthetic
18 methane. However, significant economic barriers slow down its massive deployment (e.g.
19 operating hours, expensive investments). Within this framework, the PtG-Oxycombustion
20 hybridization can palliate these issues by improving the use of resources and increasing the
21 overall efficiency. In this study we assess the requirements for electrolysis, depending on the
22 size of the oxycombustion plant, the fuel physical and chemical properties and the final
23 application of the hybrid system. Most suitable heat demanding options to implement this PtG-
24 Oxycombustion hybridization are district heating, industrial processes and small combined

Abbreviations: ASU, air separation unit; HEN, heat exchangers network; LHV, lower heating value; M, moisture; Oxy-CC, oxycombustion combined cycle; PtG, power to gas; SNG, synthetic natural gas; Z, ash.

*Corresponding author: luismi@unizar.es, Tel: +34 876 552 196, Fax: +34 976732078

25 cycled power plants. The latter case is modelled and simulated in detail and thermally
26 integrated. The global efficiency of this hybrid system increases from 56% to 68%, thanks to
27 avoiding the requirement of an air separation unit and integrating up to 88% of the available
28 heat from methanation in a LP steam cycle.

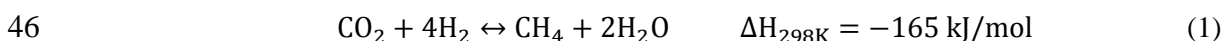
29 **Keywords**

30 Power-to-Gas, Oxycombustion, Methanation, Integration, Combined cycle

31 **1. Introduction**

32 The constant increase of electricity production from intermittent renewable energy sources has
33 brought to light the necessity of deploying energy storage systems. The management of the
34 surplus power generated by these renewable sources is crucial for developing a sustainable
35 power industry. Power-to-gas has been proposed as one of the promising technologies to
36 overcome these issues [1]. PtG technology uses electricity to produce hydrogen by electrolysis,
37 and then combines CO₂ and the produced H₂ to obtain SNG through methanation. This
38 technology widens the range of application of hydrogen as energy vector, and it makes possible
39 to produce a CO₂ neutral fuel by capturing the carbon emissions from an existing source [2][3].
40 In addition, it allows connecting the electric and gas network for increasing the flexibility of the
41 energy supply.

42 The PtG process is conceptually explained as follows: renewable electricity is converted to fuel
43 gas by means of electrolysis, storing electrical energy in form of hydrogen. Oxygen is also
44 obtained as by-product from the electrolyser. Then, the generated hydrogen is combined with
45 carbon dioxide to produce methane through the Sabatier reaction (Equation 1) [4].



47 The availability of a suitable source of CO₂ can be considered as the main limiting factor for
48 promoting PtG, since it reduces the possible geographic sites for a wide deployment of this

49 technology [5]. Biogas plants, waste managers, energy-intensive industries and power plants are
50 the largest CO₂ sources and the most interesting partners for integration with PtG [6]. However,
51 the energy consumption required to attain concentrated CO₂ streams leads to efficiency
52 penalties that range between 9-12 efficiency points [7][8], and the associated costs may vary
53 from 50 to 90 €/t_{CO₂}, depending on CO₂ concentration in flue gas and capture technology [9].
54 For this reason, some of the largest PtG projects worldwide directly upgrade biogas to obtain
55 SNG without a previous stage of CO₂ separation [10]. However, this kind of concepts makes
56 useless the byproduct oxygen coming from the electrolysis process.

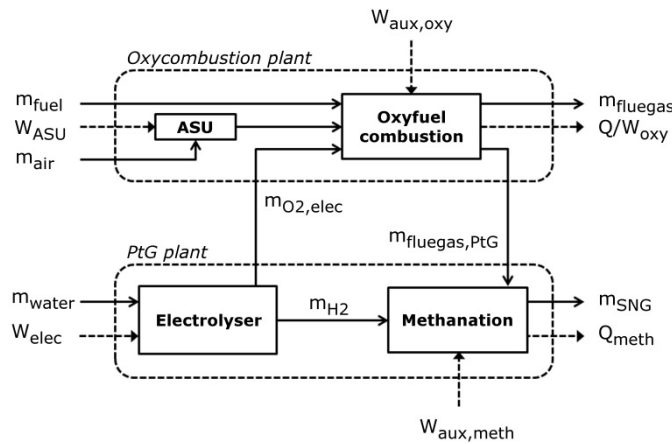
57 To this context, oxygen may be used as gasification agent or for the activation of sludge in
58 biomass gasification and sewage plants, respectively [6]. Nevertheless, the hydrogen
59 concentration in syngas from gasification may reach values above 60% and further hydrogen
60 addition is barely needed, what limits the energy storage potential [11]. Sewage plants produce
61 poor biogas and its upgrading is relatively expensive. Thus, it is currently preferred to burn this
62 gas in engines for self-consumption [12]. Hence, a suitable option to take advantage of
63 produced oxygen would be the hybridization of PtG with oxyfuel combustion. In oxyfuel
64 combustion, a mixture of pure oxygen and recycled flue gas (mainly CO₂ and H₂O) acts as
65 comburent [13]. The requirement of an air separation unit (ASU) to produce oxygen would be
66 replaced with the electrolyser which by-produces O₂. Thus, the electrical consumption of the
67 ASU would be reduced, and CO₂ would be taken from flue gas without extra energy penalty in
68 its separation. With an adequate size design of the PtG–Oxycombustion system, the by-
69 produced oxygen from electrolysis could entirely replace the ASU [6][14][15].

70 This paper deals with some potential applications that include biomass, coal and gas
71 consumption. These applications cover different sizes and technologies but all of them are based
72 on the Oxycombustion-Power to Gas hybridization. Special attention is paid to an advanced
73 oxycombustion combined cycle hybridized with PtG. This technology can achieve higher net
74 electric efficiencies [16] than air-fired coal power plants, so the required capacity of electrolysis

75 to remove the ASU is lower than in other power plants of the same net electric power.
 76 Furthermore, methanation produces extra thermal energy that can be useful. Thus, a preliminary
 77 heat integration analysis has been also performed and the maximum potential efficiency after
 78 heat integration is also determined.

79 2. Power to Gas-Oxycombustion hybridizations

80 As stated above, a suitable option to take advantage of by-produced oxygen is the hybridization
 81 of Power to Gas with oxyfuel combustion. During oxycombustion, a mixture of recycled flue
 82 gas and pure oxygen is used as comburent instead of air [17]. Thus, the large N_2 content in air is
 83 substituted by the combustion products (mainly CO_2 and H_2O), and flue gas can achieve a high
 84 carbon dioxide concentration once steam is condensed. Energy penalty associated to this capture
 85 process mainly comes from the air separation unit that produces the required oxygen with
 86 typical consumptions of 190 kWh/t_{O_2} [18]. Therefore, by using the oxygen from electrolysis we
 87 could suppress the electrical consumption of the ASU, and we would directly obtain pure CO_2
 88 for methanation from flue gas without energy penalties (Figure 1).



89

90 **Figure 1.** Scheme of the hybrid PtG-Oxycombustion concept.

91 The key variable in the Power to Gas-Oxycombustion hybridizations is the ratio that relates the
 92 chemical energy in the hydrogen from electrolysis and the net energy output of the oxyfuel
 93 combustion plant, Equation 2 (thermal outputs for boilers, ξ_{oxy} , and net electric outputs for

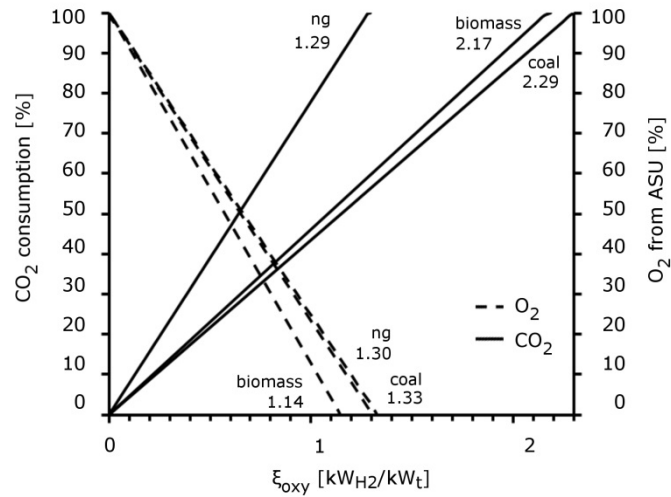
94 power plants, ξ'_{oxy}) [14][19]. The net electrical output accounts for the consumed electricity by
 95 the ASU and the auxiliary equipment in the form of Equation 3.

$$96 \quad \xi_{oxy} = \frac{LHV_{H_2} \cdot \dot{m}_{H_2}}{\dot{Q}_{oxy}} \left[\frac{kW_{H_2}}{kW_t} \right] \quad \text{or} \quad \xi'_{oxy} = \frac{LHV_{H_2} \cdot \dot{m}_{H_2}}{\dot{W}_{net,oxy}} \left[\frac{kW_{H_2}}{kW_e} \right] \quad (2)$$

$$97 \quad \dot{W}_{net,oxy} = \dot{W}_{gross,oxy} - \dot{W}_{aux,oxy} - \dot{W}_{ASU} \quad [kW_e] \quad (3)$$

98 Depending on the size ratio between the electrolyser and the oxyfuel combustion, the
 99 byproduced oxygen could cover the oxyfuel process requirements and avoid the air separation
 100 unit (situation denoted as ξ_{ASU}). Besides, whenever the installed electrolyser capacity is enough
 101 to process the whole flow of flue gas, the size ratio will be denoted as ξ_{CO_2} . The type of fuel
 102 used in oxycombustion will modify the values of ξ_{ASU} and ξ_{CO_2} (Figure 2). Thus, the use of
 103 biomass leads to lower values of ξ_{ASU} (1.14) in comparison with coal (1.33) thanks to the
 104 greater oxygen content (Table 1). Whilst the smaller C:H ratio of typical biomass fuels also
 105 gives minor values of ξ_{CO_2} (2.17) than coal (2.29) due to the less amount of CO_2 produced per
 106 generated kWh [19]. The latter effect is more pronounced for natural gas oxycombustion, thus
 107 decreasing ξ_{CO_2} (1.29) down to meet with ξ_{ASU} (1.30). Furthermore, despite of the differences
 108 between the compositions of natural gas and coal, both of them require for combustion
 109 comparable amounts of oxygen per MJ of fuel (2.80 mol_{O₂}/MJ_{fuel} for natural gas, and 2.86
 110 mol_{O₂}/MJ_{fuel} for coal, according to our simulations), what implies similar values of ξ_{ASU} .

111 It should be noted that $\xi_{CO_2} < \xi_{ASU}$ for the natural gas case, due to second order effects. Since
 112 complete combustion of CH_4 is considered and methanation is forced to be stoichiometric, the
 113 parameters ξ_{CO_2} and ξ_{ASU} should be equal for natural gas. However, second order effects
 114 modify the values of ξ , such as (a) the presence of H_2 in the fuel input (more O_2 required,
 115 $\xi_{ASU} \uparrow$), (b) the requirement of an O_2 excess during combustion (more O_2 required, $\xi_{ASU} \uparrow$),
 116 and (c) the presence of O_2 in the flow of CO_2 that is directed to methanation (more H_2 required,
 117 $\xi_{CO_2} \uparrow$). These effects almost cancel each other, and makes ξ_{ASU} slightly greater than ξ_{CO_2} .



118

119

Figure 2. Behaviour of ξ_{oxy} for coal, biomass and natural gas

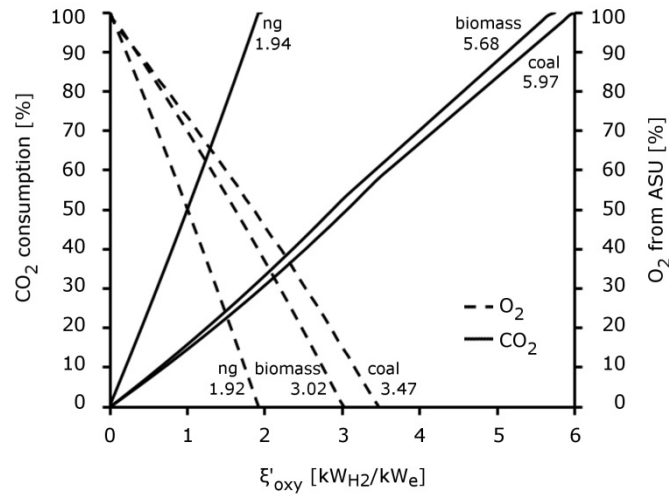
120

Table 1. Ultimate analysis of selected coal and biomass for the study [% w.b.] [14][19].

	C	H	O	N	S	M	Z	LHV [MJ/kg]
Coal	66.1	3.6	7.1	1.6	0.6	8.6	12.4	25.4
Biomass	43.9	5.5	41.6	0.3	0.0	5.5	3.2	17.8

121

122 The type of the power plant also modifies the values of ξ'_{ASU} and ξ'_{CO_2} . Figure 3 shows the
 123 behaviour of ξ'_{oxy} for a subcritical power plant with a LHV efficiency of 38.6% (coal and
 124 biomass), and for a combined cycle of 64% LHV efficiency (natural gas) [16]. The greater
 125 efficiency of the combined cycle allows reducing the amount of fuel used per kWh produced,
 126 and therefore the required oxygen for oxycombustion and the size of electrolysis.



127

128 **Figure 3.** Behaviour of ξ'_{oxy} for a subcritical power plant (coal and biomass) and a combined cycle
129 (natural gas).

130 The final application of the PtG–oxycombustion hybridization will define the adequate
131 operation point of ξ_{oxy} and ξ'_{oxy} . Five generic applications are analysed to evaluate its technical
132 feasibility. At small and mid-scale, we consider boilers producing thermal output that is applied
133 to households, district heating, or industrial processes. At big scale, we take the production of
134 electricity by combined cycles for natural gas, and by subcritical power plants for coal and
135 biomass (Table 2).

136 **Table 2.** Generic applications and characteristics for PtG-oxycombustion systems at different scales
137 (electrolyser efficiency 68.1%) [19]

<i>Thermal output</i>					
Application	\dot{Q}_{oxy} [MW]	Electrolyser [MWe]			ξ_{oxy}
		Coal	Biomass	Natural gas	
Households	0.01	0.02	0.02	0.02	$\xi_{ASU} - 1.15 \cdot \xi_{ASU}$
District heating	2	3.9 – 4.5	3.4 – 3.9	3.8 – 4.4	$\xi_{ASU} - 1.15 \cdot \xi_{ASU}$
Industry	20	39.1 – 67.3	33.5 – 63.7	39.1 – 37.9	$\xi_{ASU} - \xi_{CO2}$
<i>Electrical output</i>					
Application	$\dot{W}_{net,oxy}$ [MW]	Electrolyser [MWe]			ξ'_{oxy}
		Coal	Biomass	Natural gas	
Subcritical PP	50	350.6 – 438.3	333.6 – 417.0	–	$0.8 \cdot \xi'_{CO2} - \xi'_{CO2}$

Combined cycle	50	–	–	113.9 – 142.4	$0.8 \cdot \xi'_{\text{CO}_2} - \xi'_{\text{CO}_2}$
----------------	----	---	---	---------------	-----------------------------------------------------

138

139 Small scale installations (households and district heating) are not compelled to capture their
140 emissions since the amount of produced CO₂ is not large enough. Hence, an operation point
141 around ξ_{ASU} would be recommended. In medium scale facilities, such as industrial applications,
142 avoiding greenhouse gas emissions might be economically interesting, so they could operate in
143 the range between ξ_{ASU} and ξ_{CO_2} . Power plants should be compelled to capture their carbon
144 dioxide; therefore, a range next to ξ_{CO_2} would be the most suitable operation for those
145 applications.

146 The technical feasibility of these applications is strong limited by the high specific cost and the
147 maximum achievable size of electrolyzers. Nowadays, electrolyzers are commercially available
148 from a few kWe up to 2 MWe [20]. Therefore, coal and biomass power plants are prohibitive
149 because they require more than 160 electrolyzers. Industry and district heating are the most
150 suitable applications, since they would combine less than 30 units of 2 MWe size electrolyzers.
151 In the following section, we analyse and integrate a small combined cycle power plant as the
152 upper limit case for PtG-Oxy applications.

153 3. Power to Gas-Oxycombustion combined cycle model

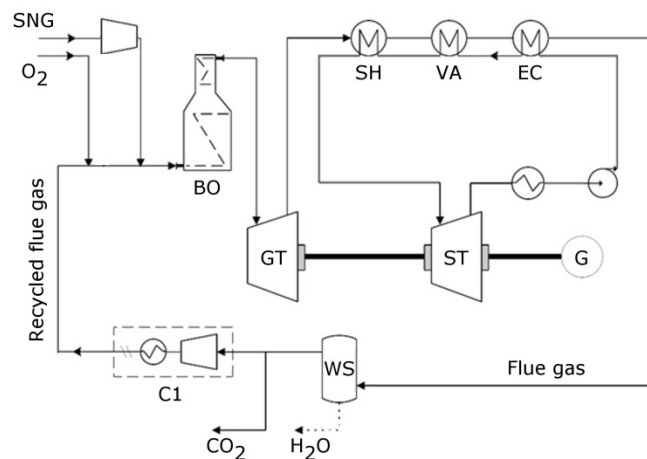
154 The operation of a Power to Gas-Oxycombustion combined cycle plant makes sense when we
155 use buffers of H₂ and O₂ to separate the storage periods from the electricity generation (the
156 analysis of storage sizing and management is beyond the scope of this paper, although it
157 becomes essential for economic analysis). Whenever renewable energy surplus exists, the
158 electrolyser starts storing this electricity as hydrogen and oxygen. Contrarily, during the periods
159 of high demand, the electrolyser remains unused, and the combined cycle generates electricity
160 using the stored oxygen for the oxycombustion. Simultaneously, the methanation process
161 combines the hydrogen with the CO₂ emissions of the power plant, what allows generating
162 approximately the same amount of SNG that is consumed. Hence, the final electricity

163 production can be considered as renewable, since methane and carbon dioxide act as the charge
164 and discharged forms of an energy carrier that is continuously recycled. Besides, the exothermal
165 heat from methanation can be integrated as low pressure steam in the steam cycle of the power
166 plant for increasing the overall efficiency.

167 The hybridization between the combined cycle in oxycombustion and the Power to Gas plant
168 has been modelled with Aspen Plus[®] under industrial conditions for steady state operation and
169 chemical equilibrium. The simulation of both plants is described in detail in the following sub-
170 sections.

171 3.1 Combined cycle power plant

172 To convert the chemical power of the produced SNG back to electric power, a gas and steam
173 cycles are combined in a single oxycombustion power plant (Oxy-CC). By burning the SNG in
174 pure oxygen, the produced flue gas is rich in CO₂ that can be easily separated from water using
175 a condenser. An overall layout of the power plant is shown in Figure 4. Pure oxygen, SNG and
176 recycled flue gas are fed to the stoichiometric combustion chamber (BO) where the temperature
177 is raised up to 1330 °C (see Table 3 for stream details). We assume a complete combustion
178 process and an isentropic efficiency of 90% for all turbines.



179

180

Figure 4. Scheme of the oxycombustion combined cycle.

181 The resulting flue gas is then expanded in a Gas Turbine (GT) to atmospheric pressure to
 182 produce about 35.7 MW_e of electric power. A Rankine cycle is then used to recover the heat
 183 from the flue gas. The Steam Turbine (ST) operates at 530°C and 150 bar and generates up to
 184 13.4 MW_e. The used Heat Recovery Steam Generator consists of 3 modules: an Economizer
 185 (EC) a Vaporizer (VA) and a Superheater (SH).

186 **Table 3.** Main streams of the oxycombustion combined cycle.

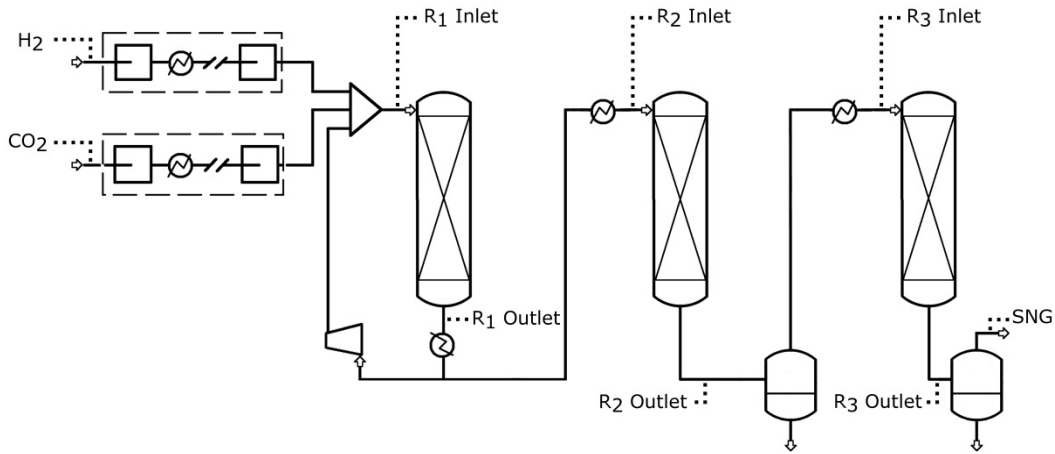
	Fuel	Comburent		Flue Gas	CO ₂ to PtG
Stream	SNG	O ₂	Recycled flue gas	Flue Gas	CO ₂
T [°C]	40.0	27	382.0	1329.5	30.0
P [bar]	26.0	40.0	40.0	40.0	1.0
Flow [Nm ³ /h]	5775.9	11210.8	67679.4	84581.4	5859.1
CO ₂ [%]	0.8	0.0	94.5	82.2	94.5
H ₂ [%]	3.5	0.0	0.0	0.0	0.0
CH ₄ [%]	95.3	0.0	0.0	0.0	0.0
H ₂ O [%]	0.4	0.0	4.3	16.8	4.3
O ₂ [%]	0.0	100.0	1.2	1.0	1.2

187

188 The total electric consumption of the Oxy-CC is the sum of the ASU consumption (3.0 MW),
 189 the multi-staged compressor of the recycle loop (13.8 MW), and the water pump in the Rankine
 190 cycle (0.2 MW). Thus, the total 49.1 MW that the plant is able to generate translates into 31.1
 191 MW of net power, assuming a 98% efficient electric generator (G). This leads to an overall
 192 plant efficiency of 55.9% defined as the ratio between the net electric output of the Oxy-CC
 193 plant (Equation 3 where $W_{aux,oxy}$ includes the consumption of the multi-staged compressor of
 194 the recycle loop) and the chemical energy contained in the SNG from PtG unit (LHV based).
 195 This value is comparable to the efficiency of NGCC power plants with CO₂ capture found in
 196 literature [21]. The Oxy-CC produces 5859.1 Nm³/h of CO₂ for methanation with 94.5 mol%
 197 CO₂ content.

198 3.2 Power to Gas plant

199 The modelled methanation facility is based on TREMP™ process from Haldor Topsøe [22], and
 200 consists of three adiabatic stages at about 30 bar with recycling on the first reactor, and a steam
 201 condenser after the second one (Figure 5). The main target is to achieve methane molar
 202 fractions above 95% in the SNG, according to the Spanish legislation [23].



203

204

Figure 5. Scheme of the Power to Gas plant.

205 The flue gas from the Oxy-CC amounts to 5859.1 Nm³/h at 30°C and 1 bar. We assume a
 206 stoichiometric methanation, so the required amount of hydrogen is 22310.1 Nm³/h. This is
 207 calculated by Equation 4 [14] as a function of the total molar flow of flue gas, \dot{n}_{FG} , and its
 208 molar concentrations of CO₂, $y_{CO_2,FG}$, and O₂, $y_{O_2,FG}$.

209
$$\dot{n}_{H_2} = 4 \cdot \left(y_{CO_2,FG} + \frac{1}{2} y_{O_2,FG} \right) \cdot \dot{n}_{FG} \quad (4)$$

210 This hydrogen comes from alkaline electrolyzers fed with renewable electricity, which have
 211 been modelled by programming a user-defined subroutine in Aspen Plus®. The inlet electric
 212 power and the inlet water stream are the initial variables for the external calculations. This block
 213 splits water in two mass flows of pure oxygen and a mixture of hydrogen with unreacted water.
 214 Based on literature, the water conversion is assumed to be 99.9% with an electrical consumption
 215 of 4.4 kWh/Nm³H₂ and an outlet temperature of 80 °C [24][25]. These operation conditions
 216 lead to an efficiency of the electrolyser unit of 68.1% (LHV basis).

217 The hydrogen and carbon dioxide are pressurized up to 30 bar prior the methanation plant. At
 218 the outlet of both compression trains, the temperature reached allows the removal of any
 219 preheating stage before the first reactor. Then, the outlet of Reactor 1 is cooled down to 300 °C,
 220 and partially recycled (72.5%) using a blower. The stream directed to the second stage of
 221 methanation enters the reactor at 250 °C. After this point, steam content strongly inhibits the
 222 methanation reaction; therefore water content is reduced to 12% through a condensation stage
 223 and the outlet gas is heated back to 250 °C prior entering the third reactor. Finally, most of the
 224 steam at the outlet of Reactor 3 is condensed, and the gas achieves SNG quality (Table 4). In the
 225 simulation, the reactor blocks calculate the composition and temperature of outlet gas streams,
 226 at equilibrium state, minimizing Gibbs free energy in an adiabatic process. Besides, the pressure
 227 drops are assumed to be 3% along the reactors and 2% in the condensation stages.

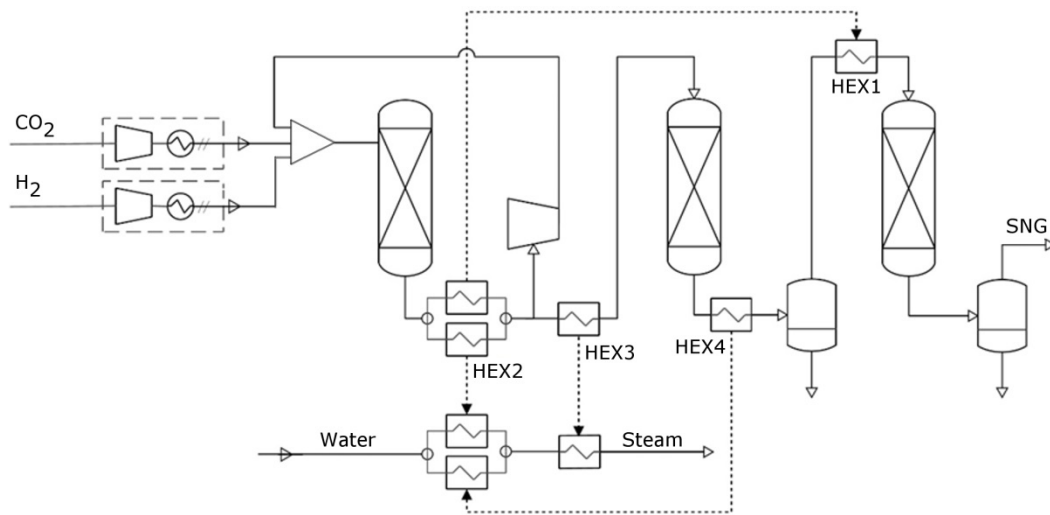
228 **Table 4.** Main streams of the Power to Gas plant.

	H ₂	CO ₂	R1 Inlet	R1 Outlet	R2 Inlet	R2 Outlet	R3 Inlet	R3 Outlet	SNG
T [°C]	80.0	30.0	307.7	592.1	250.0	421.9	250.0	366.3	40.0
P [bar]	1.0	1.0	30.0	29.1	29.1	28.2	27.7	26.8	26.3
Flow [Nm ³ /h]	22310.1	5859.1	78318.7	69143.3	18993.7	17579.7	7544.6	7090.9	5756.9
CO ₂ [%]	0.0	94.5	9.9	4.5	4.5	1.6	3.6	0.7	0.8
H ₂ [%]	99.9	0.0	41.3	20.0	20.0	6.3	14.7	2.9	3.5
CH ₄ [%]	0.0	0.0	15.3	24.0	24.0	29.9	69.7	77.3	95.2
H ₂ O [%]	0.1	4.3	32.9	50.8	50.8	62.2	12.0	19.1	0.4
CO [%]	0.0	0.0	0.5	0.7	0.7	0.0	0.0	0.0	0.0
O ₂ [%]	0.0	1.2	0.1	0.0	0.0	0.0	0.0	0.0	0.0

229 **4. Energy integration and efficiency**

230 Based on the Power to Gas plant simulation results a heat integration study is conducted in
 231 order to find the optimal Heat Exchangers Network (HEN) for heat recovery purposes. The
 232 pinch analysis methodology is integrated into the Power to Gas model in order to determine the
 233 minimal hot and cold utilities required by the process. Heat fluxes are integrated with a pinch
 234 temperature of $\Delta T=10K$ [26]. The resulting optimal HEN is shown in Figure 6. In this optimal

235 HEN, part of the heat recovered from the exit of the first reactor is used for internal heating
 236 requirements at the inlet of the third reactor (HEX1). The remaining heat is used to generate 24
 237 tonnes of LP steam per hour at 124°C and 2 bar by using 3 heat exchangers placed at the exit of
 238 the first reactor and both ends of the second (HEX2, HEX3 and HEX4).



239

240 **Figure 6.** Scheme of the Heat Exchangers Network in the methanation plant.

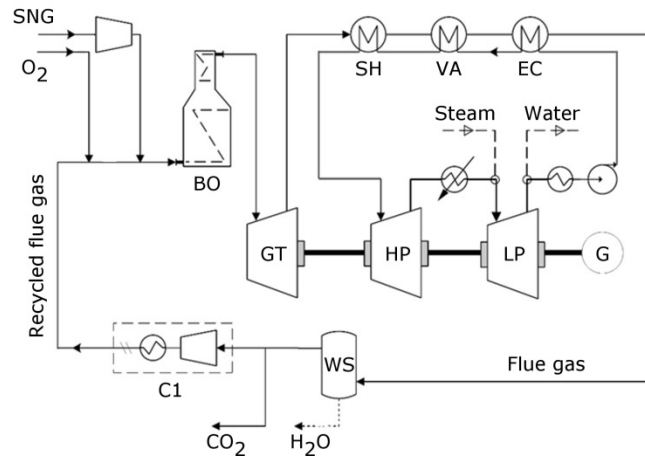
241 The heat generated at the exit of the last reactor cannot be efficiently recovered with the
 242 considered operating conditions. An external cooling utility is thus used for condensate removal
 243 from the final product (e.g. cooling tower).

244 In order to make use of this generated steam, a low pressure turbine (LP) is introduced into the
 245 previous Oxy-CC (Figure 7). The generated LP steam is mixed to the steam exiting the high
 246 pressure turbine (HP) at 2 bar before the second expansion process in the following low
 247 pressure turbine (LP). The flow exiting the LP turbine is then separated to retrieve the portion
 248 which will be pumped back to the HEN in the Power to Gas plant. This configuration allows to
 249 run the oxycombustion and Power to Gas processes separately if need be.

250 Thanks to the external heat source for more power generation (heat integration with PtG plant),
 251 the new combined cycle is able to produce 53 MW of electric power (near 8% more power).

252 The removal of ASU unit for O₂ generation avoids 3 MW of extra consumption. But the

253 requirement of a new compression train to pressurized O₂ coming from the electrolyser
 254 penalizes the system with 2.1 MW. This modification finally leads to a net power generation of
 255 35.8 MW. Thus, the total efficiency of the combined cycle rises by 11.6 points, up to 67.5%
 256 (LHV based). Moreover, the performance of the plant could still be further improved by means
 257 of an exergy analysis to identify the avoidable losses at fixed design [27].



258

259

Figure 7. Scheme of the Oxycombustion Combined Cycle heat integration.

260

5. Conclusions

261

262

263

264

265

266

267

268

269

270

271

In this study, the PtG-Oxycombustion hybridization that was presented in previous works has been assessed for different types of Oxycombustion plants. These systems store renewable electricity as hydrogen, taking also advantage of the O₂ by-produced during electrolysis to overcome the energy penalty of the ASU in an oxyfuel combustion facility. Later, the O₂ stored can be used to operate the oxycombustion plant and, in addition, the H₂ stored is used in the methanation plant to generate synthetic natural gas. The parameter used to characterize the systems is the size ratio, ξ_{oxy} , which relates the energy contained in the hydrogen from electrolysis and the net output of the oxyfuel combustion plant (thermal output for boilers, ξ_{oxy} , and net electric output for power plants, ξ'_{oxy}). Depending on the value of ξ_{oxy} , the byproduct oxygen could completely feed the oxyfuel process and avoid the air separation unit (ξ_{ASU}), or the hydrogen may be sufficient for processing the whole flow of flue gas (ξ_{CO_2}).

272 The type of fuel used in oxycombustion modifies the values of ξ_{ASU} and ξ_{CO_2} . Natural gas and
273 coal require comparable amounts of oxygen per MJ of fuel, what implies similar ξ_{ASU} (1.30 and
274 1.33, respectively), whilst biomass has greater oxygen content, thus reducing ξ_{ASU} down to
275 1.14. Besides, for smaller C/H ratios, the amount of CO_2 produced per generated kWh is lower,
276 so $\xi_{CO_2,coal} > \xi_{CO_2,biomass} > \xi_{CO_2,natural\ gas}$. The type of power plant also modifies the values
277 of ξ'_{ASU} and ξ'_{CO_2} . The lower efficiency of subcritical power plants compared to combined
278 cycles implies increasing the amount of fuel per kWh produced, the required oxygen and the
279 size of electrolysis; therefore, $\xi_{CO_2,SPP} \gg \xi_{CO_2,CC}$.

280 Five generic applications of the concept have been evaluated, from which industry and district
281 heating result the most suitable options due to their technical feasibility. Small combined cycles
282 are considered as the upper limit for PtG-Oxy applications, whilst subcritical power plants are
283 prohibitive since they require between 330 and 420 MW of electrolysis capacity. Furthermore, a
284 PtG-OxyCC hybrid system has been simulated and thermally integrated with Aspen Plus®
285 software. A total of 88% of the exothermal heat available from methanation is recovered with
286 an optimized heat exchangers network, thus generating low pressure steam that can be
287 introduced in the steam cycle of the power plant. Hence, the absence of ASU unit for O_2
288 generation and the use of the methanation heat allow increasing the overall efficiency from
289 55.9% to 67.5%.

290 **Acknowledgements**

291 This research is co-funded by the University of Zaragoza, Fundación Bancaria Ibercaja, and
292 Fundación CAI, through the program “Programa Ibercaja-Cai Estancias de Investigación”
293 (project ‘Storage of surplus renewable electricity: Cross-border collaboration between France
294 and Spain for developing Power-to-Gas technology’). Financial support for M. Bailera during
295 his Ph.D. studies was co-funded by the Department of Industry and Innovation of Diputación
296 General de Aragón, and by the European Social Fund.

297 **Nomenclature**

Variables

LHV	Lower heating value [kJ/kg]
\dot{m}	Mass flow [kg/s]
\dot{n}	Molar flow [kmol/s]
P	Pressure [bar]
\dot{Q}	Thermal power [kWt]
T	Temperature [°C]
W	Electric power [kWe]
y	Molar fraction [-]
ξ_{oxy}	Ratio between electrolyser and boiler outputs [kWe/kWt]
ξ'_{oxy}	Ratio between electrolyser and power plant outputs [kWe/kWt]

Subscripts

ASU	Air separation unit
aux	Auxiliary consumption
CC	Combined cycle
CO_2	Carbon dioxide
FG	Flue gas
$gross$	Gross power
H_2	Hydrogen
net	Net power
oxy	Oxycombustion plant
O_2	Oxygen
SPP	Subcritical power plant

298

299 **References**

- 300 [1] Scamman D, Newborough M. Using surplus nuclear power for hydrogen mobility and
 301 power-to-gas in France. *Int J Hydrogen Energy* 2016;41:10080–9.
 302 doi:10.1016/j.ijhydene.2016.04.166.
- 303 [2] Streibel M, Nakaten N, Kempka T, Kühn M. Analysis of an integrated carbon cycle for
 304 storage of renewables. *Energy Procedia* 2013;40:202–11.
 305 doi:10.1016/j.egypro.2013.08.024.
- 306 [3] Kühn M, Nakaten N, Streibel M, Kempka T. CO₂ geological storage and utilization for a
 307 carbon neutral “power-to-gas-to-power” cycle to even out fluctuations of renewable
 308 energy provision. *Energy Procedia* 2014;63:8044–9. doi:10.1016/j.egypro.2014.11.841.
- 309 [4] Estermann T, Newborough M, Sterner M. Power-to-gas systems for absorbing excess
 310 solar power in electricity distribution networks. *Int J Hydrogen Energy* 2016;41:13950–
 311 9. doi:10.1016/j.ijhydene.2016.05.278.
- 312 [5] Schneider L, Kötter E. The geographic potential of Power-to-Gas in a German model
 313 region-Trier-Amprion 5. *J Energy Storage* 2015;1:1–6. doi:10.1016/j.est.2015.03.001.
- 314 [6] Sterner M. Bioenergy and renewable power methane in integrated 100% renewable
 315 energy systems. Kassel university press GmbH, 2009.
- 316 [7] Goto K, Yogo K, Higashii T. A review of efficiency penalty in a coal-fired power plant
 317 with post-combustion CO₂ capture. *Appl Energy* 2013;111:710–20.
 318 doi:10.1016/j.apenergy.2013.05.020.

- 319 [8] Thambimuthu K, Soltanieh M, Abanades JC. Capture of CO₂. IPCC Spec. Rep. Carbon
320 dioxide Capture Storage, Cambridge University Press; 2005, p. 105–78.
- 321 [9] Rubin ES, Davison JE, Herzog HJ. The cost of CO₂ capture and storage. *Int J Greenh*
322 *Gas Control* 2015;40:378–400. doi:10.1016/j.ijggc.2015.05.018.
- 323 [10] Bailera M, Lisbona P, Romeo LM, Espatolero S. Power to Gas projects review: Lab,
324 pilot and demo plants for storing renewable energy and CO₂. *Renew Sustain Energy Rev*
325 2017;69:292–312. doi:10.1016/j.rser.2016.11.130.
- 326 [11] Iskov H, Rasmussen NB. Global screening of projects and technologies for Power-to-
327 Gas and Bio-SNG. Danish Gas Technology Centre; 2013.
- 328 [12] Szwaja S, Kovacs VB, Bereczky A, Penninger A. Sewage sludge producer gas enriched
329 with methane as a fuel to a spark ignited engine. *Fuel Process Technol* 2013;110:160–6.
330 doi:10.1016/j.fuproc.2012.12.008.
- 331 [13] Toftegaard MB, Brix J, Jensen PA, Glarborg P, Jensen AD. Oxy-fuel combustion of
332 solid fuels. *Prog Energy Combust Sci* 2010;36:581–625.
333 doi:10.1016/j.pecs.2010.02.001.
- 334 [14] Bailera M, Lisbona P, Romeo LM. Power to gas-oxyfuel boiler hybrid systems. *Int J*
335 *Hydrogen Energy* 2015. doi:10.1016/j.ijhydene.2015.06.074.
- 336 [15] Spazzafumo G. Storing renewable energies in a substitute of natural gas. *Int J Hydrogen*
337 *Energy* 2016;41:19492–8. doi:10.1016/j.ijhydene.2016.05.209.
- 338 [16] Climent Barba F, Martínez-denegri Sánchez G, Soler Seguí B, Gohari Darabkhani H,
339 John Anthony E. A technical evaluation, performance analysis and risk assessment of
340 multiple novel oxy-turbine power cycles with complete CO₂ capture. *J Clean Prod*
341 2016;133:971–85. doi:10.1016/j.jclepro.2016.05.189.
- 342 [17] Wall T, Liu Y, Spero C, Elliott L, Khare S, Rathnam R, et al. An overview on oxyfuel
343 coal combustion-State of the art research and technology development. *Chem Eng Res*
344 *Des* 2009;87:1003–16. doi:10.1016/j.cherd.2009.02.005.
- 345 [18] Hu Y, Li X, Li H, Yan J. Peak and off-peak operations of the air separation unit in oxy-
346 coal combustion power generation systems. *Appl Energy* 2013;112:747–54.
347 doi:10.1016/j.apenergy.2012.12.001.
- 348 [19] Bailera M, Lisbona P, Romeo LM, Espatolero S. Power to Gas–biomass oxycombustion
349 hybrid system: Energy integration and potential applications. *Appl Energy* 2015.
350 doi:10.1016/j.apenergy.2015.10.014.
- 351 [20] Sharma S, Ghoshal SK. Hydrogen the future transportation fuel: From production to
352 applications. *Renew Sustain Energy Rev* 2015;43:1151–8.
353 doi:10.1016/j.rser.2014.11.093.
- 354 [21] Kanniche M, Gros-Bonnivard R, Jaud P, Valle-Marcos J, Amann J BC. Pre-combustion,
355 Post-combustion and Oxy-combustion in thermal power plant for CO capture. *Appl*
356 *Therm Eng* 2009;30:53.
- 357 [22] Kopyscinski J, Schildhauer TJ, Biollaz SM a. Production of synthetic natural gas (SNG)
358 from coal and dry biomass - A technology review from 1950 to 2009. *Fuel*
359 2010;89:1763–83. doi:10.1016/j.fuel.2010.01.027.
- 360 [23] BOE-A-2013-185. Resolución de 21 de diciembre de 2012, de la Dirección General de
361 Política Energética y Minas, por la que se modifica el protocolo de detalle PD-01.
362 Ministerio de Industria, Energía y Turismo; 2013.
- 363 [24] Tijani AS, Yusup NAB, Rahim a. HA. Mathematical Modelling and Simulation
364 Analysis of Advanced Alkaline Electrolyzer System for Hydrogen Production. *Procedia*

365 Technol 2014;15:799–807. doi:10.1016/j.protcy.2014.09.053.

366 [25] Dieguez P, Ursua a, Sanchis P, Sopena C, Guelbenzu E, Gandia L. Thermal
367 performance of a commercial alkaline water electrolyzer: Experimental study and
368 mathematical modeling. *Int J Hydrogen Energy* 2008;33:7338–54.
369 doi:10.1016/j.ijhydene.2008.09.051.

370 [26] De Saint Jean M, Baurens P, Bouallou C, Couturier K. Economic assessment of a power-
371 to-substitute-natural-gas process including high-temperature steam electrolysis. *Int J*
372 *Hydrogen Energy* 2015;40:6487–500. doi:10.1016/j.ijhydene.2015.03.066.

373 [27] Hagi H, Le Moullec Y, Nemer M, Bouallou C. Performance assessment of first
374 generation oxy-coal power plants through an exergy-based process integration
375 methodology. *Energy* 2014;69:272–84. doi:10.1016/j.energy.2014.03.008.

376

377

378

379 **List of figures**

380 Figure 1: Scheme of the hybrid PtG-Oxycombustion concept

381 Figure 2: Behaviour of ξ_{oxy} for coal, biomass and natural gas

382 Figure 3: Behaviour of ξ'_{oxy} for a subcritical power plant (coal and biomass) and a combined
383 cycle (natural gas)

384 Figure 4: Scheme of the oxycombustion combined cycle

385 Figure 5: Scheme of the Power to Gas plant

386 Figure 6: Scheme of the Heat Exchangers Network in the methanation plant

387 Figure 7: Scheme of the Oxycombustion Combined Cycle heat integration

388

389 **List of tables**

390 Table 1: Ultimate analysis of selected coal and biomass for the study [%w.b.] [14][19]

391 Table 2: Generic applications and characteristics for PtG-oxycombustion systems at different
392 scales (electrolyser efficiency 68.1%) [19]

393 Table 3: Main streams of the oxycombustion combined cycle

394 Table 4: Main streams of the Power to Gas plant